

Effect of tension and curvature on the chemical potential of lipids in lipid aggregates†

Cite this: *Phys. Chem. Chem. Phys.*, 2013, **15**, 876

Andrea Grafmüller,* Reinhard Lipowsky and Volker Knecht

Understanding the factors that influence the free energy of lipids in bilayer membranes is an essential step toward understanding exchange processes of lipids between membranes. In general, both lipid composition and membrane geometry can affect lipid exchange rates between bilayer membranes. Here, the free energy change ΔG_{des} for the desorption of dipalmitoyl-phosphatidylcholine (DPPC) lipids from different lipid aggregates has been computed using molecular dynamics simulations and umbrella sampling. The value of ΔG_{des} is found to depend strongly on the local properties of the aggregate, in that both tension and curvature lead to an increase in ΔG_{des} . A detailed analysis shows that the increased desorption free energy for tense bilayers arises from the increased conformational entropy of the lipid tails, which reduces the favorable component $-T\Delta S_L$ of the desorption free energy.

Received 29th August 2012,
Accepted 14th November 2012

DOI: 10.1039/c2cp43018e

www.rsc.org/pccp

Introduction

Lipid bilayers belong to the most important structural elements of biological cells, and combine structural stability with great flexibility. The remarkable mechanical properties of these aggregates arise from a delicate balance of hydrophobic forces and molecular interactions within the membrane.¹ Membranes in different compartments within cells can vary strongly in both lipid composition and shape. Lipid transport between the different compartments is required to maintain and control these different compositions. In the cell, this may take place by monomeric lipid exchange or through vesicular transport.² For vesicular transport, the desorption of single lipid tails represents an important first step on the way to vesicle fusion.^{3–5} Monomeric lipid exchange in turn can occur spontaneously or involve lipid transfer proteins (LTP) to facilitate the process.²

Despite their low solubility, spontaneous exchange of lipids between membranes can also be observed in experiments of pure lipid bilayer membranes^{6–8} and is known to depend on both membrane curvature and the membrane composition.^{6,9–11} Moreover, it was recently observed that the rate of monomeric lipid exchange from tightly packed lipid nano-discs was much greater than that from large unilamellar vesicles (LUV).¹²

At low membrane concentrations, lipid exchange between membranes is likely to take place *via* desorption and diffusion of the lipid, where the desorption process is the rate limiting step.^{7,10} Depending on the concentration, an activation–collision process, in which the lipid partially desorbs and thus facilitates the exchange in a collision between two membranes may also take place.¹³ In both cases, fluctuations of the lipid out of the membrane plane play a role. The likelihood of such fluctuations is determined by the associated free energy change of the lipid.

Molecular dynamics (MD) simulations offer a convenient tool to investigate the details of such fluctuations. However, due to the low solubility of typical lipids, large fluctuations cannot be observed in unbiased equilibrium simulations. A series of recent papers have used umbrella sampling simulations to calculate the potential of mean force (PMF) acting on a lipid for displacement normal to the membrane for a number of different lipid types.^{14–18}

To elucidate how factors such as the different local structure, lipid packing and composition affect lipid exchange, a better understanding of the role of different contributions to the desorption free energy is required. Membrane tension,¹⁹ the membrane affinity of peptides^{20,21} and molecular association^{22,23} have been shown to depend on a delicate balance of large contributions with opposite sign. The desorption free energy of lipids is related to the first moment of the internal pressure of these aggregates,¹ and thus likely to be affected in a similar manner.

Here we use atomistic MD simulations with umbrella sampling to obtain the PMFs for the desorption of dipalmitoyl-phosphatidylcholine (DPPC) lipids from bilayer membranes at

Max Planck Institute for Colloids and Interfaces, 14424 Potsdam, Germany.

E-mail: gmueller@mpikg.mpg.de; Fax: +49 (0)331 5679612;

Tel: +49 (0)331 567 9619

† Electronic supplementary information (ESI) available. See DOI: 10.1039/c2cp43018e

zero and finite tension, as well as from a spherical micelle as an extreme case of an aggregate with a very high local curvature. These calculations reveal a strong dependence of the desorption free energy on the local membrane geometry. A detailed analysis suggests that in bilayer structures the conformational entropy of the lipid chains at different bilayer tension is the major contribution to this dependence, while in the spherical micelle the even larger entropy difference is in part compensated by the effect of other interactions.

Computational methods

MD simulations were used to compute desorption free energies for the following systems: (a) a tension free DPPC bilayer, (b) a DPPC bilayer at a lateral pressure of -40 bar and (c) a spherical micelle. The details of the setup and conditions of all simulated systems are described below.

All simulations were performed in the NPT ensemble using the GROMACS molecular dynamics package,²⁴ version 3.3.1. The temperature was kept at 323 K by separately coupling lipids and water to a heat bath *via* the Berendsen scheme²⁵ with a relaxation time of 0.1 ps; the average pressure was likewise controlled using the Berendsen scheme with a relaxation time of 1.0 ps. In simulations of membranes, the box dimensions parallel and normal to the bilayer were scaled independently while in the simulations of a micelle the ratio of sidelengths was kept constant. The overall center of mass motion of each system was removed.

Lipids and water molecules were described using parameters from Berger *et al.*²⁶ and the simple point charge (SPC) model,^{27–29} respectively. A 1 nm cutoff for Lennard-Jones parameters was used, and full electrostatic interactions were evaluated using the particle mesh Ewald technique^{30,31} with a cutoff distance of 1 nm in direct space, 0.12 nm grid spacing and a 4th order polynomial. Covalent bonds in the lipids were constrained using LINCS³² while water molecules were kept rigid with SETTLE,³³ allowing the use of a 4 fs timestep.

The system setup for the bilayer simulations consists of a bilayer patch containing 64 DPPC lipids hydrated by 3846 SPC water molecules under periodic boundary conditions. With no lateral tension this corresponds to a $4.6 \times 4.6 \times 9.5$ nm³ simulation box. Micelle simulations contain a micelle with 23 lipids surrounded by 13 089 water molecules, corresponding to a simulation box size of $6.6 \times 6.6 \times 10.2$ nm³. The number of lipids was chosen such that the diameter of the micelle is roughly equal to the bilayer thickness.

For potential of mean force (PMF) calculations a harmonic umbrella potential was applied to the phosphate group of one of the lipids. Consequently, its spatial coordinate z relative to the center-of-mass of the unrestrained lipids in the direction perpendicular to the bilayer served as a reaction coordinate. For the micelle simulations, the position of the pulled lipid in the xy -plane was also restrained with respect to the position of the micelle, while, similar to that for the bilayer, the z coordinate of the phosphate group relative to the center-of-mass of the micelle served as the reaction coordinate. Starting configurations

for each window were created with 1 ns simulations using an umbrella potential with a lower force constant of 500 kJ mol⁻¹ nm⁻² and subsequently equilibrated for 10 ns with a final force constant of 5000 kJ mol⁻¹ nm⁻². Data were collected from 100 ns simulations, and the weighted histogram analysis method³⁴ was used to construct the PMF from the biased distribution. Standard errors for the PMFs were obtained by dividing the trajectories into four blocks and calculating the standard deviation between the four profiles. For that purpose the PMFs were aligned by setting the free energy of the equilibrium position to zero.

For each bilayer system, 61 umbrella windows between $z = 1$ nm and a distance of $z = 4$ nm away from the center-of-mass of the bilayer were simulated, so that the spacing between two consecutive windows was 0.05 nm. For the micelle, 49 umbrella windows between $z = 1.6$ nm and $z = 4$ nm were used.

To improve the accuracy of the desorption free energies, additional PMF profiles were calculated, in which the umbrella potential was applied to the final carbon groups of both lipid tails while the phosphate group was restrained at a fixed value of $z = 3.1$ nm. Here 46 equally spaced umbrella windows for the corresponding reaction coordinate z_{ta} were sampled for 50 ns, with values of z_{ta} between $z_{\text{ta}} = 0.8$ nm and $z_{\text{ta}} = 3.5$ nm.

Results and discussion

Configurations from a bilayer and a micelle simulation are shown in Fig. 1(a and b). When a lipid is pulled away from its

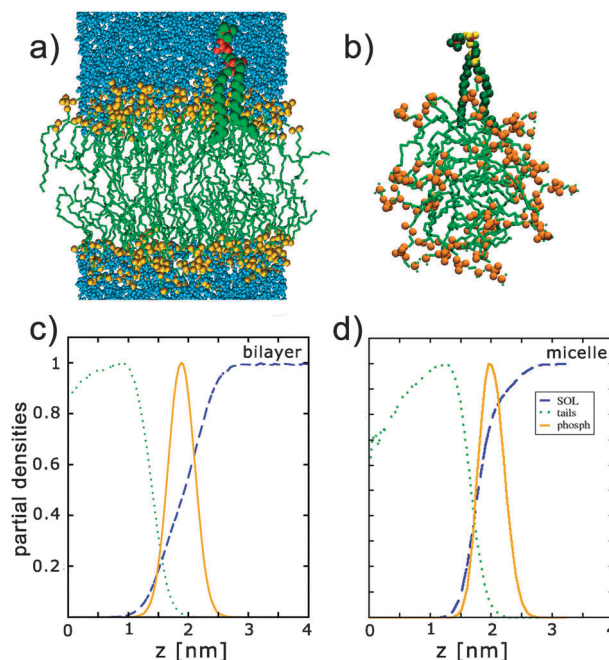


Fig. 1 Configurations of the simulations of a relaxed bilayer (a) and a spherical micelle (b), respectively, as well as the normalized number density of heavy atoms for lipid tails (green), phosphate groups (orange) and solvent molecules (blue) as a function of the distance from the center of the bilayer (c) and the micelle (d).

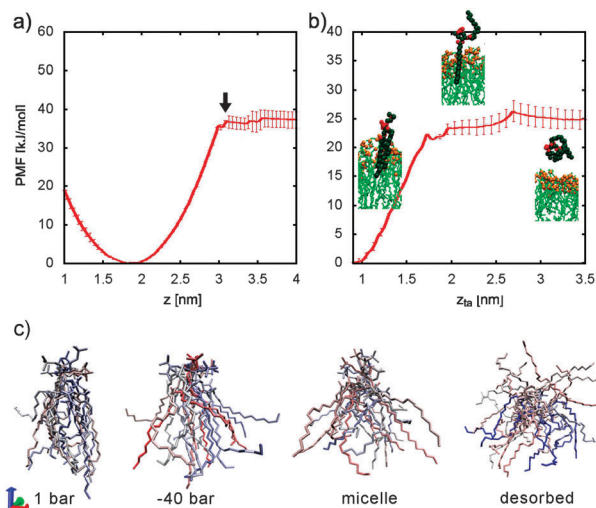


Fig. 2 Potential of mean force along (a) the position z of a DPPC phosphate group relative to the bilayer center and (b) the position z_{ta} of the final two carbon atoms of the same lipid for $z = 3.1$ nm. The insets show snapshots of the lipid corresponding to the different parts of the PMF profile. (c) Superimposed configurations of lipids at their equilibrium z position in the tension-free bilayer, the tense bilayer and the micelle as well as for a lipid restrained in solution, illustrating the conformational space sampled by the lipid tails. Conformations are taken from the last 50 ns of the simulations and superimposed at the phosphate group by simple translation.

equilibrium position and out of the membrane, it will eventually desorb from the bilayer and be completely solvated. The corresponding PMF profile in Fig. 2(a) shows a steep increase in the free energy as the lipid is pulled, which levels out to a plateau as soon as the lipid is completely desorbed and thus does not feel the presence of the membrane anymore. The free energy value corresponding to this plateau has been used in a number of studies to estimate the desorption free energy of lipids, and the results were shown to give a reasonable agreement with experimental extrapolation from lipids with short hydrocarbon of the critical micelle concentration (CMC).^{14,16}

The desorption free energy estimated in this way from the PMF depends critically on the point of desorption of the tails, due to the steep increase in the free energy with z . However, sampling this point correctly poses a challenge to simulations, because in its vicinity the lipid tails will have a finite probability for both the adsorbed and the free state. The driving force for tail adsorption is the hydrophobic effect of the tails, whereas the free state is stabilized by the gain in chain entropy when the – at that point almost completely stretched¹⁴ – tails in the adsorbed state take up a more compact conformation in solution as in Fig. 2(c). Transitions between these states are observed on timescales ≥ 100 ns. Therefore, simulations will not be able to sample the equilibrium distribution of the tails close to their desorption point. This may lead to the observation of large error bars in the plateau region and to discrepancies between different PMF simulations. Note that the error bars indicated in Fig. 2(a) represent the standard deviation obtained from the 100 ns trajectories. The real error due to the

bias from the initial state is likely to be larger (based on the results described below it is on the order of 25 kJ mol^{-1}).

To overcome the sampling problem associated with the position of the lipid tails, the center-of-mass position of the final hydrocarbons of the two chains relative to the bilayer center has been introduced as a second reaction coordinate z_{ta} . The value of z_{ta} was varied for a fixed value of $z = 3.1$ nm, indicated by an arrow in Fig. 2, for which the unbiased tails are always inserted in the membrane so that the PMF(z) has a well defined value at this point. As z_{ta} increases from its equilibrium position, initially the two hydrocarbons have on average the same distance from the bilayer center. When z_{ta} becomes large enough to be in the headgroup region, it becomes energetically favorable to keep one tail inserted as far as the position of the head group allows, while the second tail is desorbed from the membrane.

This corresponds to two distinct regions in the corresponding PMF shown in Fig. 2(b). The free energy increases steeply until the first tail is desorbed. After desorption of the first tail the profile remains flat as long as one tail remains inserted in the bilayer, while the solvated one rotates further away from the membrane. Finally, the second tail also desorbs corresponding to a small second increase in free energy. Snapshots of the corresponding lipid conformations are shown in the insets in Fig. 2(b).

The total desorption free energy corresponds to the free energy cost of first moving the lipid to $z = 3.1$ nm and then desorbing the tails. For a tension free membrane, the free energy of pulling the lipid from its equilibrium position to $z = 3.1$ nm is found to be 37 kJ mol^{-1} or $14 k_{\text{B}}T$. The free energy cost to pull both tails out of the bilayer at position $z = 3.1$ nm is 26 kJ mol^{-1} or $10 k_{\text{B}}T$, so that the desorption free energy is found to be $\Delta G_{\text{des}} = 63(\pm 4) \text{ kJ mol}^{-1}$ or $24 k_{\text{B}}T$. This is in fair agreement with the estimate of 69 kJ mol^{-1} or $26 k_{\text{B}}T$ derived from the CMC, although somewhat smaller than previous simulation results.¹⁴

Using the same protocol to determine the free energy change upon desorption of a lipid from a tense bilayer with a lateral pressure $P_{\text{lat}} = -40$ bar, we find a value of $80(\pm 2) \text{ kJ mol}^{-1}$. This is 17 kJ mol^{-1} or $7 k_{\text{B}}T$ larger than that for the desorption from the relaxed bilayer. Closer inspection of the two contributions in Fig. 3 shows that this difference is related to the first part of the desorption process, *i.e.* pulling the lipid headgroup from its equilibrium position to $z = 3.1$ nm. The free energy change of pulling the tails out of the membrane is very similar to that found for the relaxed membrane.

A likely explanation of these observations is the changed conformational entropy of the lipid tails in the tense membrane and the micelle relative to the relaxed membrane suggested by the snapshots in Fig. 2c and Fig. 4 in ref. 14. When the lipid is pulled away from its equilibrium position and into solution, its tails, which are extended within a conical region in the bilayer, become disordered with random orientations, which corresponds to an increase in conformational entropy. This represents a favorable contribution to lipid desorption and partially compensates the unfavorable increase in free energy

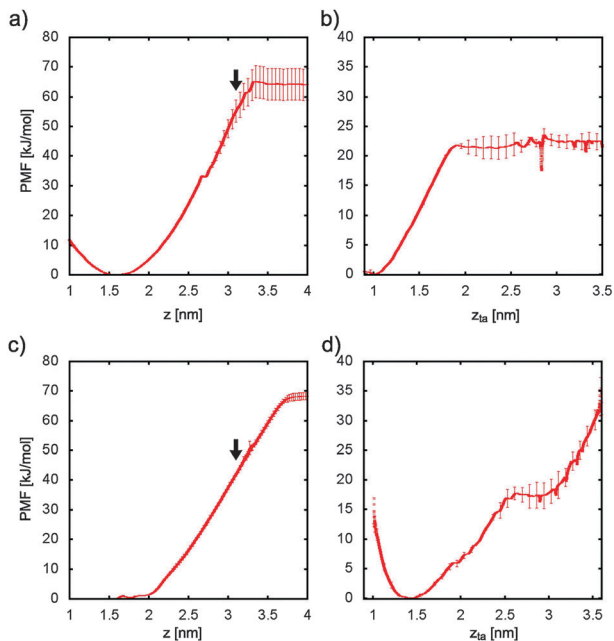


Fig. 3 PMF profiles for lipid desorption from a tense bilayer (a and b) and a micelle (c and d). Panels (a) and (c) show the free energy profile of moving the DPPC phosphate group to position z and panels (b) and (d) the free energy of desorbing the tails at position $z = 3.1$ nm marked by an arrow in (a) and (c).

associated with exposing the unpolar lipid tails to the water. In the tense bilayer the lipids are more disordered and thus have a higher conformational entropy in the aggregates and consequently the entropy gain of the lipids in solution is smaller here.

To investigate the effect of the local structure on desorption further, the free energy change of desorption of a lipid from a spherical micelle containing 23 lipids has been determined by the same procedure. Such an aggregate has a very high local curvature, and strongly perturbed lipid structure, as might be found at the edge of a bilayer or near a localized pore defect. Lipid tails are even more disordered than in the tense bilayer. As expected, the desorption free energy for the micelle has increased compared to the relaxed bilayer and is found to be $\Delta G_{\text{des,m}} = 73(\pm 1.3)$ kJ mol⁻¹ or $28(\pm 0.5) k_{\text{B}}T$. The difference is however smaller than that for the tense membrane.

For a quantitative assessment of these effects, the free energy change is divided into the contributions arising from changes in the lipid entropy $-T\Delta S_{\text{L}}$ and all other contributions ΔG_{R} according to

$$\Delta G_{\text{des}} = \Delta G_{\text{R}} - T\Delta S_{\text{L}}. \quad (1)$$

In particular, here we have estimated the average conformational entropy S_{X} of individual lipids in the different aggregates using the mass-weighted covariance matrix for the transferred lipid together with the quasi-harmonic (QH) approximation.³⁵ Similarly, the average entropy of the lipid in solution $S_{\text{L,W}}$ is determined to give the change in lipid entropy, as it is transferred from a bilayer to solution, $\Delta S_{\text{L}} = S_{\text{L,W}} - S_{\text{X}}$, where S_{X} can stand for the conformational entropy S_0 of a lipid in a relaxed

Table 1 Thermodynamic quantities for the transfer of a DPPC lipid from an aggregate into water for a bilayer at zero tension (bilayer), a bilayer with a lateral pressure of -40 bar (tension), and a spherical micelle (micelle). Listed are the free energy for lipid desorption from the PMF calculations, ΔG_{des} , its shift with respect to the bilayer at zero tension, $\Delta\Delta G_{\text{des}}$, the change in the entropy of the transferred lipid obtained from the quasi-harmonic approximation, $-T\Delta S_{\text{L}}$, and the entropy difference of a lipid in one of the aggregates and the bilayer at zero tension, $-T\Delta\Delta S_{\text{L}}$. All free energy estimates are given in kJ mol⁻¹

	ΔG_{des}	$\Delta\Delta G_{\text{des}}$	$-T\Delta S_{\text{L}}$	$-T\Delta\Delta S_{\text{L}}$
Bilayer	63(± 2)	0	-67(± 3)	0
Tension	80(± 2)	17(± 3)	-50(± 6)	14(± 5)
Micelle	73(± 1.3)	10(± 3)	-19(± 6)	55(± 5)

membrane, S_{σ} in a tense membrane or S_{m} in a micelle. The shift in the free energy of desorption that stems from the changed lipid entropy in the aggregate is given by $-T\Delta\Delta S_{\text{L}} = -T(\Delta S_{\text{X}} - \Delta S_0)$, which depends only on the lipid entropies in the aggregates, according to

$$-T\Delta\Delta S_{\text{L}} = -T(S_{\text{X}} - S_0), \quad (2)$$

thus reducing the statistical error. The results of this analysis are summarized in Table 1. The change in the desorption free energy is $\Delta\Delta G_{\text{des}} = 17(\pm 3)$ kJ mol⁻¹ for the tense membrane, which is in good quantitative agreement with $-T\Delta\Delta S_{\text{L}} = 14(\pm 5)$ kJ mol⁻¹. The change in the desorption free energy can therefore be well explained by the conformational entropy change of the lipids in the tense bilayer. The contribution of the conformational entropy of lipids in the spherical micelle on the other hand is found to be 55 kJ mol⁻¹ larger than in the relaxed bilayer, whereas the desorption free energies only differ by ≈ 10 kJ mol⁻¹. Although the QH method is an approximation, the differences in entropy for the three different aggregates agree with the expectation that the conformational freedom of the tails increases in the tense bilayer compared to the relaxed one and becomes even larger in the micelle. This expectation is also confirmed by the results of a previous study using the QH method on different lipids, which found that effects due to anharmonicity and higher order correlations are small for these systems.³⁶

It appears that the large difference in conformational entropy is to a large part compensated by other contributions of ΔG_{R} to the free energy. ΔG_{R} includes the enthalpy change of the system, ΔH , and other entropic contributions of the remaining lipids, ΔS_{LR} , and the solvent, ΔS_{sol} , which contributes greatly to the hydrophobic effect.³⁷ The energy change due to the hydrophobic effect will be related to the number of contacts between water molecules and the hydrophobic chains. The number of such contacts, and its change after desorption, was measured for the three different aggregates. A contact is defined by a distance smaller than the first minimum at 0.56 nm in the radial distribution function (shown in Fig. S1, ESI[†]). Contact numbers are listed in Table 2. The numbers show that while a lipid in the tense bilayer has only few additional contacts with water molecules, compared to a relaxed bilayer, the number of tail-water contacts for a lipid in the micelle is approximately 5 times as high. The number of

Table 2 Number of contacts N_{tw} per lipid between lipid tails and water molecules for a bilayer at zero tension (bilayer), a bilayer with a lateral pressure of -40 bar (tension), a spherical micelle (micelle) and a solvated lipid (lipid). Only closest contacts are counted, so that each water atom contributes only one contact. $N_{tw,des}$ and $\Delta N_{tw,agg}$ denote the number of contacts in the aggregate after desorption and the change to the unperturbed state, respectively. $\Delta N_{tw,lipid}$ is the change in tail–water contacts of the desorbed lipid

	N_{tw}	$N_{tw,des}$	$\Delta N_{tw,agg}$	$\Delta N_{tw,lipid}$
Bilayer	12.3(± 0.3)	10.5(± 0.5)	-1.8(± 0.6)	291(± 19)
Tension	16.0(± 0.5)	12.7(± 0.6)	-3.3(± 0.8)	287(± 19)
Micelle	61.4(± 1.8)	64.7(± 0.9)	3.3(± 2)	242(± 20)
Lipid	303(± 19)			

tail–water contacts per lipid within the aggregates also changes little on desorption. However, when desorbed, the lipid gains approximately 290(± 19) contacts in the case of the relaxed bilayer, but only 242(± 20) for the micelle. This difference may lead to a reduced contribution of water–chain interactions to the desorption free energy and thus partially compensates the larger entropy change found for the micelle. It is further likely that the total enthalpy ΔH in the systems will change on desorption. However, due to the many degrees of freedom of the solvent molecules, the enthalpy of the total systems converges slowly and large statistical errors remain in the estimates. A similar trend is reflected in those estimates, which predict that the difference between the tense and the relaxed bilayer $\Delta\Delta H_{\sigma} = 12(\pm 90)$ kJ mol $^{-1}$ lies within the (large) statistical error, whereas for the micelle the enthalpy change $\Delta\Delta H_m$ is $-2700(\pm 110)$ kJ mol $^{-1}$. However, these values are not precise enough for a quantitative evaluation.

Finally, a factor that may contribute to the different desorption free energies for the bilayer structures is the asymmetry between the two leaflets after the lipid has been pulled out, which will lead to different elastic tensions in the two monolayers, due to the small system size. To estimate whether this results in a significant contribution, the area compressibility modulus K_A has been obtained from the slope of the tension vs. area diagram³⁸ (shown in Fig. S2, ESI †), which is 283 dyn cm $^{-1}$ for the tension-free bilayer and 111 dyn cm $^{-1}$ in the vicinity of $P_{lat} = -40$ bar. Using the assumption that the K_A for each monolayer is approximately $K_A/2$ in the expression for the elastic energy of stretching per area³⁹ $\omega_s = (1/2)K_A(\Delta A/A_0)^2$ and inserting the measured values of A/lipid for the two monolayers, we find that the magnitude of this contribution to the desorption free energy is on the order of 2.9(± 1.0) kJ mol $^{-1}$ for the relaxed and $-1.0(\pm 1.7)$ kJ mol $^{-1}$ for the tense bilayer. Both values are relatively small compared with the observed effect. If the desorption free energies are corrected by these contributions, the agreement with the QH result improves even further.

The large values for the enthalpy changes and the large negative total contribution of $-T\Delta S_L = -67$ kJ mol $^{-1}$ to the desorption free energy from the relaxed bilayer, which is similar to the magnitude of the desorption free energy itself, suggest that the free energy of desorption arises from a balance of opposite contributions each of which is larger than the net

effect itself. The negative term is overcompensated by positive contributions from ΔG_R . As ΔG_{des} arises from a subtle balance of opposing interactions, it is plausible to be highly susceptible to changes in conditions.

A similar subtle balance between large opposite contributions for lipid assemblies was already found to play a role in the membrane tension, making it very susceptible to small force field differences.¹⁹ It appears therefore reasonable that the same should be true for the desorption free energy of lipids, which is related to the local pressure profile.

Further evidence for the effect of lipid chain entropy was described in recent experiments for the exchange of lipids from LUVs and from lipid disks, in which the lipids are more compressed,¹² where the desorption was found to be sensitive to lipid packing. The desorption rate of lipids from the disks was found to be 20 fold faster than from LUVs.

In previous simulation of bilayers containing DPPC and cholesterol, an increase in the cholesterol content was observed to lead to a decrease in the size of the desorption free energies of DPPC.¹⁵ As cholesterol is known to increase the order of lipid chains, the decrease in the magnitude of ΔG_{des} for more ordered chains is in agreement with this study. For monolayers containing DPPC, DOPC, and cholesterol, no effect of the cholesterol concentration on ΔG_{des} was observed, however, the order parameter of the lipid chains was also found to be unaffected,¹⁸ so that in that case there would also be no entropy difference of the lipids to produce the changed ΔG_{des} . In general however, a similar effect of the area per molecule on the desorption free energy would be expected also for Langmuir monolayers at densities similar to that in the bilayers. All of these observations are consistent with the results described here.

In conclusion, our analysis of the desorption free energy of lipids from different lipid aggregates points to a number of factors, which affect lipid exchange. It appears that one of the main factors contributing to the difference is the conformational entropy of the lipid's hydrophobic chains. The more ordered the lipid packing is in the aggregate, the larger is the entropy gain upon desorption, and the lower is the desorption free energy. Thus the lipid's entropy gain on desorption partially compensates the unfavorable contribution from the hydrophobic effect. However, as the results for the micelle show, other contributions such as the number of water contacts and changes in the enthalpy also play a role. What is clear from these three systems is that the local structure has a strong influence on the free energy of lipids in the aggregates. In view of this influence, it would also be of interest to study the effects of other local membrane deformations, such as the compression of tails in a curved bilayer or a lipid disk, in order to further elucidate the free energy changes involved in lipid exchange.

Acknowledgements

The authors thank Y. Smirnowa, S. J. Marrink, D. Bennett, and D. P. Tieleman for valuable discussions.

References

- 1 D. Marsh, *Biochim. Biophys. Acta Biomembr.*, 1996, **1286**, 183–223.
- 2 S. Lev, *Nat. Rev. Mol. Cell Biol.*, 2010, **11**, 739–750.
- 3 A. Grafmüller, J. Shillcock and R. Lipowsky, *Phys. Rev. Lett.*, 2007, **98**, 218101.
- 4 A. Grafmüller, J. Shillcock and R. Lipowsky, *Biophys. J.*, 2009, **96**, 2658–2675.
- 5 Y. G. Smirnova, S.-J. Marrink, R. Lipowsky and V. Knecht, *J. Am. Chem. Soc.*, 2010, **132**, 6710–6718.
- 6 J. D. Jones and T. E. Thompson, *Biochemistry*, 1990, **29**, 1593–1600.
- 7 L. R. McLean and M. C. Phillips, *Biochemistry*, 1981, **20**, 2893–2900.
- 8 L. R. McLean and M. C. Phillips, *Biochemistry*, 1984, **23**, 4624–4630.
- 9 F. Jähnig, *Biophys. J.*, 1984, **46**, 687–694.
- 10 J. W. Nichols and R. E. Pagano, *Biochemistry*, 1981, **20**, 2783–2789.
- 11 L. R. McLean and M. C. Phillips, *Biochim. Biophys. Acta Biomembr.*, 1984, **776**, 21–26.
- 12 M. Nakano, M. Fukuda, T. Kudo, M. Miyazaki, Y. Wada, N. Matsuzaki, H. Endo and T. Handa, *J. Am. Chem. Soc.*, 2009, **131**, 8308–8312.
- 13 T. L. Steck, F. J. Kezdy and Y. Lange, *J. Biol. Chem.*, 1988, **263**, 13023–13031.
- 14 D. P. Tieleman and S. J. Marrink, *J. Am. Chem. Soc.*, 2006, **128**, 12462–12467.
- 15 W. F. Drew Bennett, J. L. MacCallum and D. P. Tieleman, *J. Am. Chem. Soc.*, 2009, **131**, 1972–1978.
- 16 N. Sapay, W. F. D. Bennett and D. P. Tieleman, *Soft Matter*, 2009, **5**, 3295–3302.
- 17 N. Sapay, W. F. D. Bennett and D. P. Tieleman, *Biochemistry*, 2010, **49**, 7665–7673.
- 18 C. Laing, S. Baoukina and D. P. Tieleman, *Phys. Chem. Chem. Phys.*, 2009, **11**, 1916–1922.
- 19 E. Lindahl and O. Edholm, *J. Chem. Phys.*, 2000, **113**, 3882–3893.
- 20 C. von Deuster and V. Knecht, *Biochim. Biophys. Acta Biomembr.*, 2011, **1808**, 2867–2876.
- 21 C. von Deuster and V. Knecht, *Biochim. Biophys. Acta Biomembr.*, 2012, **1818**, 2192–2201.
- 22 V. Knecht, *J. Phys. Chem. B*, 2010, **114**, 12701–12707.
- 23 P. Kar, R. Lipowsky and V. Knecht, *J. Phys. Chem. B*, 2011, **115**, 7661–7669.
- 24 D. van der Spoel, E. Lindahl, B. Hess, G. Groenhof, A. E. Mark and H. J. C. Berendsen, *J. Comput. Chem.*, 2005, **26**, 1701–1718.
- 25 H. Berendsen, J. Postma, W. van Gunsteren, A. Di Nola and J. Haak, *J. Chem. Phys.*, 1984, **81**, 3684–3690.
- 26 O. Berger, O. Edholm and F. Jähnig, *Biophys. J.*, 1997, **72**, 2002–2013.
- 27 H. J. C. Berendsen, J. P. M. Postma, W. F. van Gunsteren and J. Hermans, *Intermolecular Forces*, D. Reidel Publishing Company, Dordrecht, 1981, pp. 331–342.
- 28 W. Jorgensen, J. Chandrasekhar, J. Madura, R. Impey and M. Klein, *J. Chem. Phys.*, 1983, **79**, 926–935.
- 29 J. Hermans, H. J. C. Berendsen, W. F. van Gunsteren and J. P. M. Postma, *Biopolymers*, 1984, **23**, 1513–1518.
- 30 T. Darden, D. York and L. Pedersen, *J. Chem. Phys.*, 1993, **98**, 10089–10092.
- 31 U. Essmann, L. Perera, M. L. Berkowitz, T. Darden, H. Lee and L. G. Pedersen, *J. Chem. Phys.*, 1995, **103**, 8577–8593.
- 32 B. Hess, H. Bekker, H. J. C. Berendsen and J. G. E. M. Fraaije, *J. Comput. Chem.*, 1997, **18**, 1463–1472.
- 33 S. Miyamoto and P. A. Kollman, *J. Comput. Chem.*, 1992, **13**, 952–962.
- 34 S. Kumar, D. Bouzida, R. Swendsen, P. Kollman and J. Rosenberg, *J. Comput. Chem.*, 1992, **13**, 1011–1021.
- 35 I. Andricioaei and M. Karplus, *J. Chem. Phys.*, 2001, **115**, 6289.
- 36 R. Baron, A. H. de Vries, P. H. Huenenberger and W. F. van Gunsteren, *J. Phys. Chem. B*, 2006, **110**, 15602–15614.
- 37 H. S. Frank and M. W. Evans, *J. Chem. Phys.*, 1945, **13**, 507–532.
- 38 R. Goetz and R. Lipowsky, *J. Chem. Phys.*, 1998, **108**, 7397–7409.
- 39 W. Helfrich, *Z. Naturforsch., C: Biochem., Biophys., Biol., Virol.*, 1973, **28**, 693.